A small molecule inhibitor of RNA-binding protein IGF2BP3 shows anti-leukemic activity

Amit K. Jaiswal,[1] Georgia M. Scherer,[2+] Michelle L. Thaxton,[1+] Jacob P. Sorrentino,[2] Constance Yuen,[3] Milauni M. Mehta,[2] Gunjan Sharma,[1] Tasha L. Lin,[1] Tiffany M. Tran,[1] Amanda Cohen,[1] Alexander J. Ritter,[4] Rishi S. Kotecha,[5-7] Jeremy R. Sanford,[4,8] Robert D. Damoiseaux,[3,9-11] Neil K. Garg[2] and Dinesh S. Rao[1,11,12]

[1]Department of Pathology and Laboratory Medicine, University of California, Los Angeles, CA, USA; [2]Department of Chemistry and Biochemistry, University of California, Los Angeles, CA, USA; [3]California Nanosystems Institute, University of California, Los Angeles, CA, USA; [4]Department of Molecular, Cell and Developmental Biology and Center for Molecular Biology of RNA, University of California, Santa Cruz, CA, USA; [5]Department of Clinical Haematology, Oncology, Blood and Marrow Transplantation, Perth Childrens Hospital, Perth, Western Australia, Australia; [6]Leukemia Translational Research Laboratory, WA Kids Cancer Centre, University of Western Australia, Perth, Western Australia, Australia; [7]Curtin Medical School, Curtin University, Perth, Western Australia, Australia; [8]Center for Biomolecular Science & Engineering, University of California, Santa Cruz, CA, USA; [9]Department of Molecular and Medical Pharmacology, University of California, Los Angeles, CA, USA; [10]Department of Bioengineering, Samueli School of Engineering, University of California, Los Angeles, CA, USA; [11]Jonsson Comprehensive Cancer Center, University of California, Los Angeles, CA, USA and [12]Broad Stem Cell Research Center, University of California, Los Angeles, CA, USA

[+]*GMS and MLT contributed equally.*

Correspondence: D.S. Rao
drao@mednet.ucla.edu

Received: May 14, 2025.
Accepted: November 18, 2025.
Early view: November 27, 2025.

https://doi.org/10.3324/haematol.2025.288221

Jaiswal et al., 2025

Supplemental Files Table of Contents

Supplementary Figure 1.

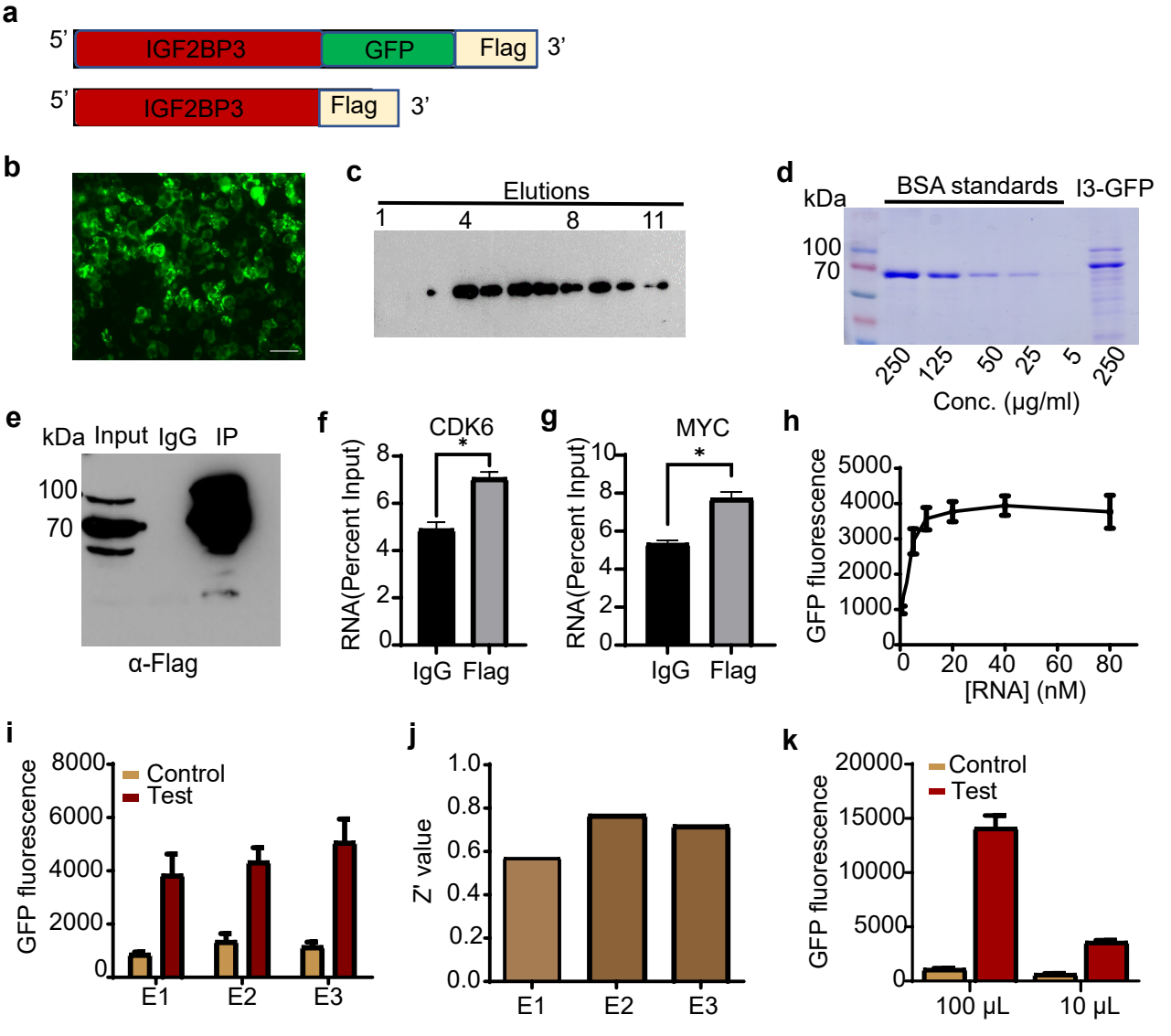

Supplementary Figure 2.

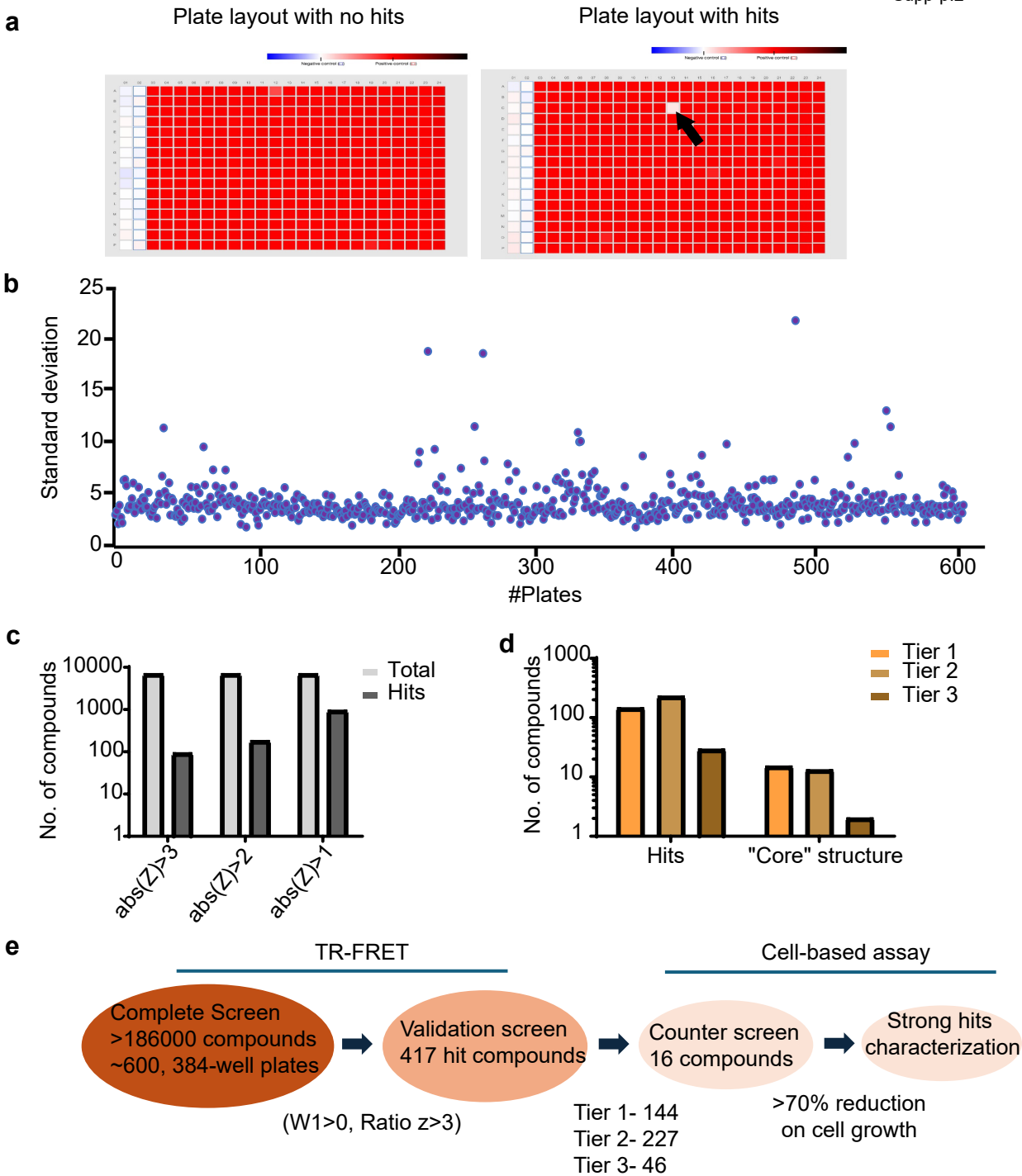

Supplementary Figure 3.

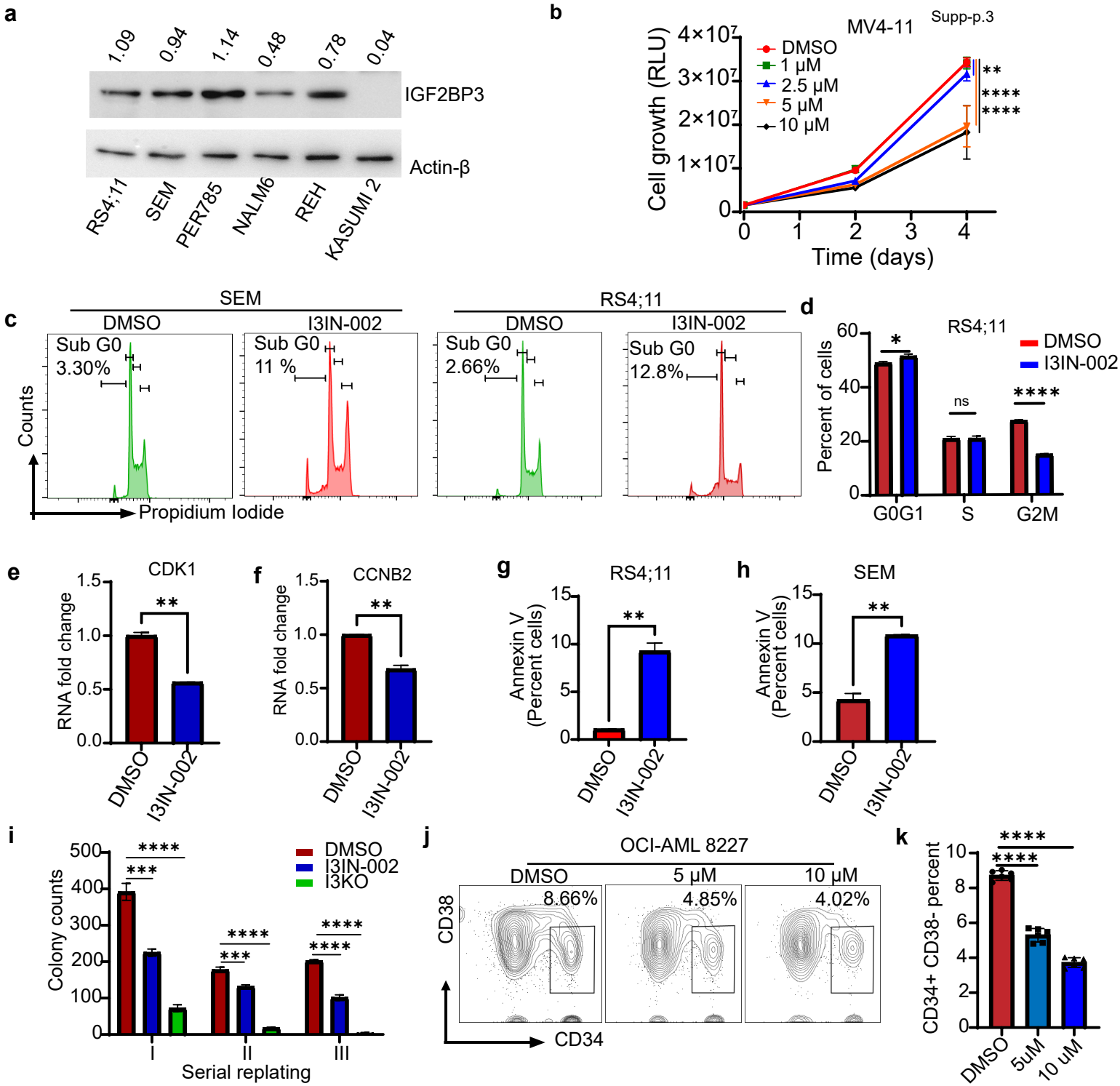

Supplementary Figure 4.

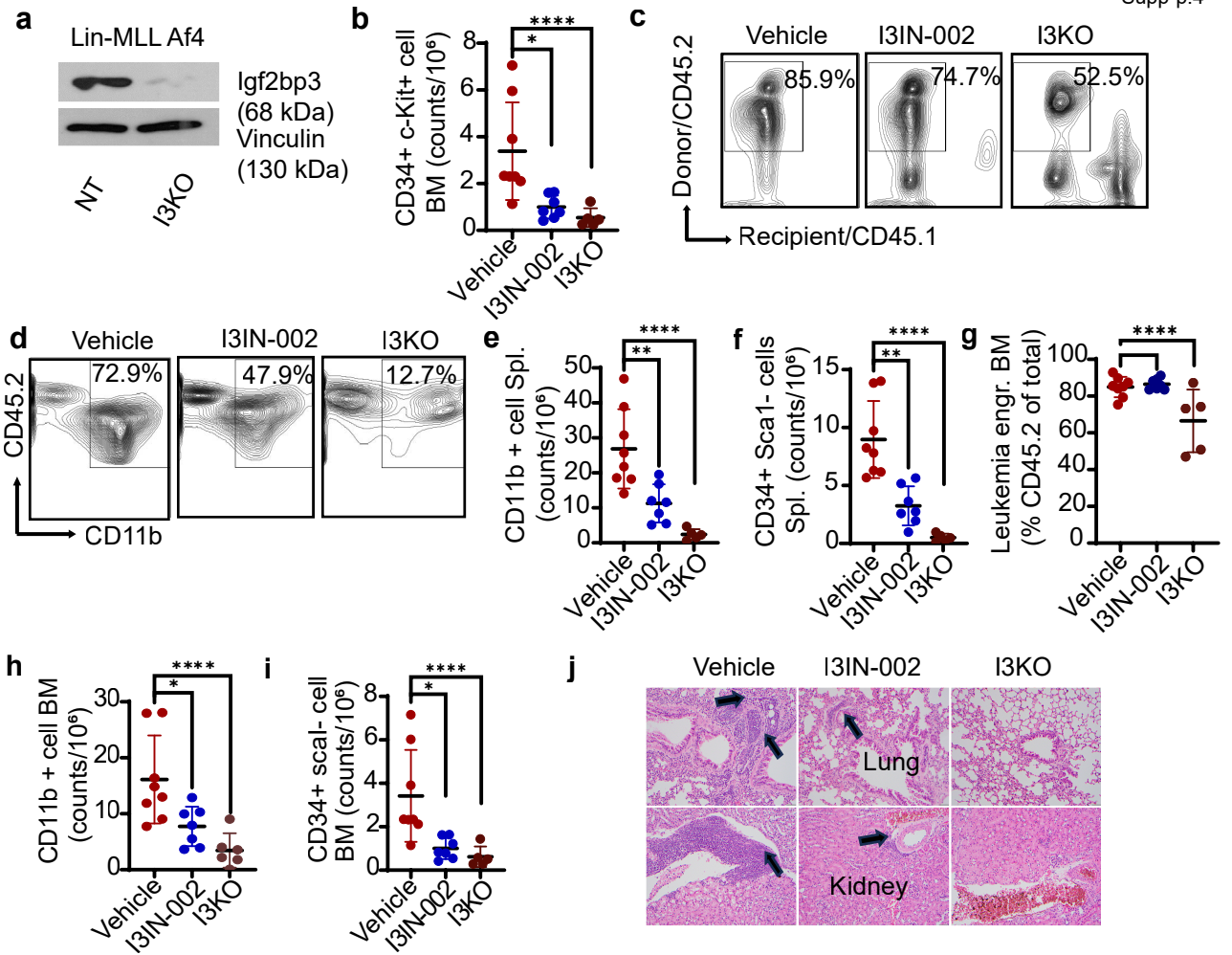

Supplementary Figure 5.

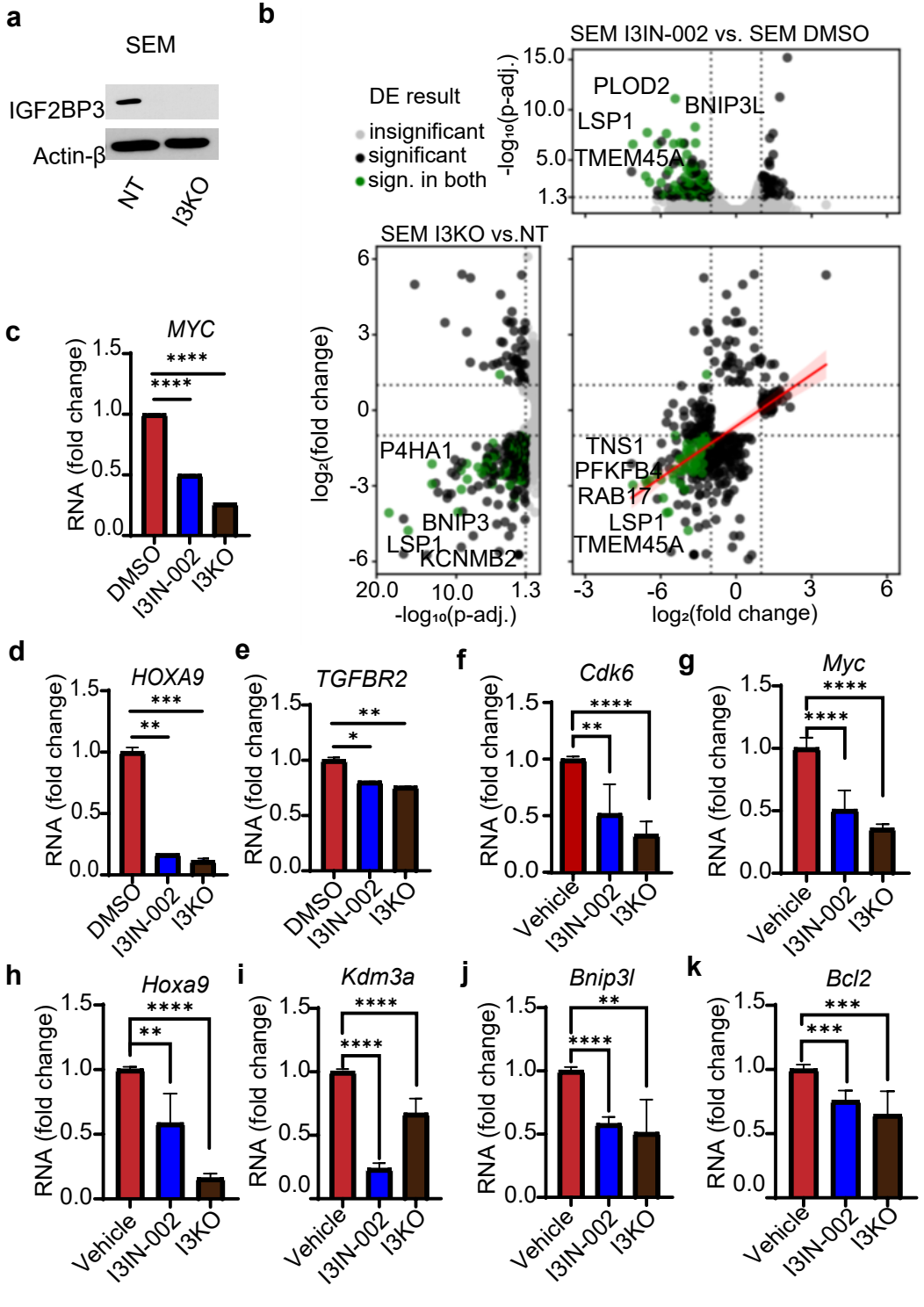

Supplementary Figure 6.

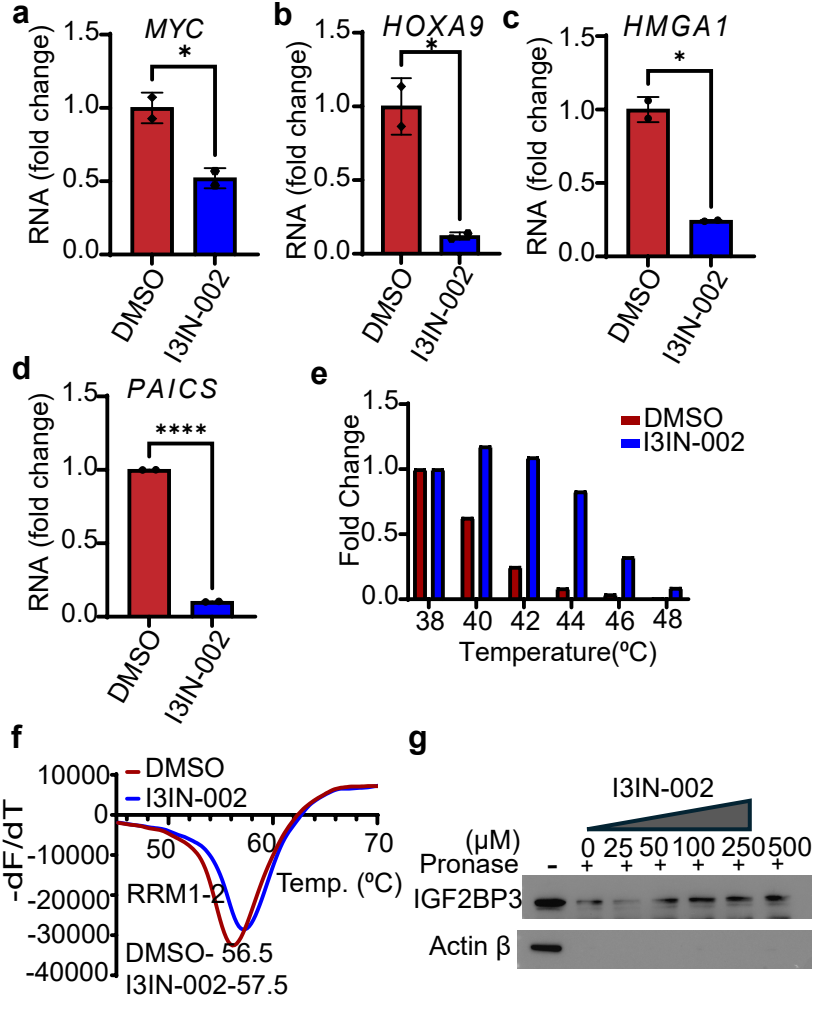

Supplemental Figure Legends.

Supplemental Figure 1, related to Figure 1. Configuration and standardization of TR-FRET assay.

a. Schematic representation of constructs used in protein purification for TR-FRET.

b. Photomicrograph of GFP fluorescence following transfection of plasmid. Scale bar, 50 micron.

c. Western blot analysis for IGF2BP3 in elutions from anti-Flag column.

d. Coomassie stained polyacrylamide gel showing I3-GFP purified from the column.

e-g. RNA immunoprecipitation using purified IGF2BP3 protein (confirmed by Western Blot), (e) of *CDK6* (f) and *MYC* (g) mRNAs, assessed by RT-qPCR.

h. GFP Fluorescence (arbitrary units) as a function of RNA oligonucleotide concentration.

i-j. GFP fluorescence and Z' values in three different experiments performed on three different days (E1-E3; n=110 (replicates); assay volume= 10 µL)

k. Comparison of GFP fluorescence in 100 µL and 10 µL assay volume**.**

Supplemental Figure 2. High throughput screening assay, related to Figure 1.

a. Plate layout and example plate with hit (right). Please see materials and methods for further details.

b. Plot of plate standard deviations across 600+ plates used for the assay.

c. Number of compounds identified as hits by different cut-off criteria in preliminary screening experiment. Based on established literature and these results a cut-off of $|z|>3$ was chosen.

d. To confirm hits identified in the full-scale screen, several replicate experiments were carried out to assess changes in fluorescence ratios. 417 high-probability hits were re-pinned into two 384-well plates and were subjected to the same TR-FRET assay as before. An individual compound was defined as being a "hit" in the validation screen when the fluorescence ratio deviated from negative controls by greater than three standard deviations. Next, we defined a

Tier 1 hit compound as positive in both experimental replicates; Tier 2 hit compound as positive in 1 out of 2 experimental replicates, and Tier 3 compounds were “non-hits” in the validation experiment based on their not being positive in either replicate. The relative frequency of Tier 1, Tier 2 and Tier 3 compounds amongst all “primary hits” versus amongst compounds with “Core structure” are plotted here.

e. Overall strategy of TR-FRET screen, validation, and counter-screen.

Supplemental Figure 3. Characterization of anti-leukemic effects of I3IN-002, related to Figure 3 and Figure 4.

a. Baseline expression of IGF2BP3 in B-ALL and AML cells.

b. Concentration dependent alterations of cell growth curves over 4 days of cell culture with I3IN-002 treatment, assessed by CellTiterGlo assay, and plotted as relative luminescence units (RLU) in MV4-11.

c. FACS-based cell cycle analysis following treatment with I3IN-002 versus control, with histograms of propidium iodide staining in SEM and RS4;11 cells.

d. Quantification of percentage of RS4;11 cells at each stage of cell cycle with 3 replicates.

e-f. G2-M transition genes CDK1 and CCNB2 downregulated in I3IN-002 treatment.

g-h. Quantitation of total Annexin V positivity in RS4;11 and SEM cells following treatment with I3IN-002. Data represents mean and standard error of mean with 3 replicates.

i. Decreased colony counts upon serial replating in different treatment groups

j-k. FACS histogram and quantitation, respectively, of a leukemic stem-cell enriched population by assaying the CD34+ CD38- population following in vitro treatment of OCI-AML-8227 cells in culture.

Supplemental Figure 4. Further characterization of in vivo phenotypes related to Figure 5.

a. Western blot showing Igf2bp3 expression in NT and Igf2bp3 knockout Lin- MLL- Af4 cells.

b. Absolute counts of CD34+ cKit+ leukemic cell in bone marrow compartment.

c. FACS histograms of CD45.1/CD45.2 congenic marker staining for measurement of leukemia engraftment.

d. FACS histograms of CD45.2/CD11b staining for measurement of leukemia engraftment.

e-f. Absolute counts of CD11b and CD34+ Sca1- cells in spleen compartments.

g. Percent quantification of Leukemic engraftment in the bone marrow.

h-i. Absolute counts of CD11b and CD34+ Sca1- cells in bone marrow compartments.

j. Histologic sections of lung and kidney comparing the morphology of tissues following engraftment of leukemia and treatment with vehicle, I3IN-002, or genetic deletion of IGF2BP3. Arrows show areas of leukemic infiltration. Hematoxylin and eosin staining, original magnification, 200X.

Supplemental Figure 5. Characterization of on-target activity of IGF2BP3, related to Figure 6.

a. IGF2BP3 expression in NT and IGF2BP3 KO SEM cells.

b. Volcano plots of differentially expressed genes with genetic IGF2BP3 knockout (left) and with I3IN-002 treatment (top) in SEM cells, using DESeq analysis on RNA-sequencing data from SEM cells treated with DMSO, I3IN-002 and SEM/I3KO.

c-d. RT-qPCR analysis for *MYC* and *HOXA9* from RNA immunoprecipitation sample..

e. RT-qPCR of additional genes *TGFBR2* identified from differential expression analyses of RNA-sequencing experiments.

f-k. RT-qPCR analyses of RNA isolated from mouse spleen following in vivo treatment described in **Fig. 5**. Three representative mice from each group were selected for the RT-qPCR analyses.

Supplemental Figure 6. **Characterization of on-target activity of IGF2BP3, related to Figure 6.**

a-d. RT-qPCR analysis for *MYC*, *HOXA9, HMGA1 and PAICS* from RNA immunoprecipitation sample.

e. Quantification of Western blot bands from Cellular thermal shift assay.

f. Thermal shift assay on purified RRM 1-2 domain of IGF2BP3.

g. Drug affinity responsive target stability show I3IN-002 protects IGF2BP3 from Pronase activity.

Detailed description of Methods

Cell lines and cell culture

All cell lines were maintained in standard conditions in incubator at 37 °C and 5% CO_2. Human B-ALL cell lines, RS4;11 (ATCC CRL-1873), NALM6 (ATCC CRL-3273), SEM (DMZ-ACC 546), PER785 , REH (ATCC CRL-8286), MV4;11 (ATCC CRL-9591), and KASUMI 2 (DSMZ ACC 526) were cultured as previously described (1-4). Immortalized MLL-Af4 transformed hematopoietic stem and progenitor cells derived from mouse bone marrow (MLL-Af4 Lin- cells) were cultured in IMDM with 15% FBS, supplemented with recombinant mouse stem cell factor (SCF, 100 ng/mL, Thermo Fisher), recombinant mouse Interleukin-6 (IL-6, 4 ng/mL, Thermo Fisher), recombinant human FMS like tyrosine kinase 3 ligand (FLT3-L, 50 ng/mL, Thermo Fisher) and mouse thrombopoietin (TPO,50 ng/mL, Thermo Fisher). OCI-AML8227 cells were a kind gift from Dr. John Dick and Dr. Eric Lechman (5). OCI-AML 8227 cells were cultured in a specialized media AMEM (Wisent Bio), BITS 9000 (Stem Cell Technologies), stem cell factor (SCF, 200 ng/mL, R&D systems), thrombopoietin (TPO, 25 ng/mL, R&D systems), FMS like tyrosine kinase 3 ligand (FLT3-L, 50 ng/mL, R&D systems), Interleukin-6 (IL-6, 20ng/mL, R&D systems), interleukin-3 (IL-3, 10 ng/mL, R&D systems), granulocyte Colony- Stimulating Factor (G-CSF, 10 ng/mL, R&D systems). OCI-AML8227 cells were cultured by plating 450000 cells/well of non-tissue culture treated 24-well plate (Eppendorf co.) and were passaged every 7 days. These are further listed in **Supp. Table 1**.

CRISPR/Cas9-mediated deletion of IGF2BP3 in cell lines

Human B-ALL cell lines SEM, RS4;11, and NALM6 were depleted for IGF2BP3 using lentiviral delivery of CRISPR/Cas9 components in a two-vector system and sgRNA sequence as previously described (1, 6). Immortalized MLL-Af4 Lin- cells were initially isolated from bone marrow of Cas9-GFP mice and then transformed using retroviral transduction with MLL-Af4 retroviral supernatant, with four rounds of transduction with MLL-Af4 retroviral supernatant, followed by selection in G418

supplemented media at 400 µg/mL for 7 days, as previously described. Cells were then stably transduced with lentiviral supernatant containing sgRNA against *Igf2bp3* (I3Cr2) or non-targeting (NT-1), and sorted on GFP and mCherry positivity (1, 6).

Protein over-expression and purification

IGF2BP3-GFP-Flag over-expression plasmid was constructed by fusing full length IGF2BP3 CDS with GFP CDS and cloned in pCDNA 3.0 vector. pCDNA3/IGF2BP3.GFP.Flag construct was transfected in 293T cells plated in 150 mm tissue culture dish. After 48 hours of transfection, cells were lysed in non-denaturing lysis buffer (50 mM Tris- HCl, pH 7.4, 300 mM NaCl, 5% glycerol, 0.1% NP40, 1X DNase, 10 units RNase/mL, 7.0 mg/50 mL of DTT, 1x Protease inhibitor) and incubated on ice for 1 hour. followed by 25 cycles of sonication with 10 seconds. 'on' and 20 seconds. 'off' pulse. Lysate was cleared by centrifugation at 12,000 x g for 15 minutes. Cleared lysates were loaded in the column filled with Anti-FLAG M2 resin (Sigma Aldrich) and passed multiple times to assist the binding. The bound protein fraction was eluted by adding 0.5 M Glycine HCl, pH 3.5 buffer. The eluent was concentrated using Vivaspin MwCO 50 column (Greiner Bio One). The concentrated protein was stored in 100 mM Tris-HCl buffer at pH 7.2. The purity and integrity of the protein was determined by mass spectroscopy and SDS-PAGE Commassie staining. The specificity of the purified protein was determined by western blotting and probing for IGF2BP3 using rabbit Anti-human IGF2BP3 antibody.

Protein extraction and Western blot

Cell lysates were made in non-denaturing cell lysis buffer and RIPA lysis buffer. Lysates were electrophoresed using SDS-PAGE using standard conditions (7). A comprehensive list of antibodies is provided in **Supp. Table 2**.

TR-FRET assay

TR-FRET assay was performed using the purified IGF2BP3-GFP fusion protein**.** Briefly, FRET assay was performed in assay buffer (50mM Tris-HCl, pH 7.4, 150 mM NaCl, DTT, 5% Glycerol, protease inhibitor (1x), RNase Inhibitor (10u/mL)). First, the purified protein was diluted at 50 nM concentration (2x) in the assay buffer and added to the plate. In the second step, 20 nM (2x) concentration of biotinylated M6A labelled RNA oligo (**Supp. Table 3**) was incubated with Streptavidin-Terbium in the assay buffer for 30 mins. on ice. After the incubation was over, the Streptavidin-Tb + RNA complex was added to the wells with purified proteins. The plate was incubated for 1 hr. at RT for binding and read on EnVision microplate reader (Perkin Elmer) with a dual PMT configuration using a 340 nm excitation and a dual emission mirror block with using a 495 nm emission filter for Terbium fluorescence (W1 channel) and a 525 nm emission filter for GFP fluorescence (W2 channel). The measurement details were as follows: 2000 cycles, 120 flashes, 200 us delay and 300 us total time window. Excitation and emission light were set to 100%. The assay was miniaturized to 10uL in 384-well plates and an in-house compound deck at UCLA MSSR was applied to the assay, with parameters as described in Results.

Data analysis of HTS assays

Values for W2, W1 and the ratio of W2 to W1 for each compound, DMSO and no IGF2BP3-GFP controls were imported into our Collaborative Drug Discovery platform for each plate and Z' for each plate determined. Z'<0.5 were flagged for repeats. Plates were normalized for Teribum (W1), GFP (W2) and W2/W1 ratios (Ratio), prospective hits were flagged for further analysis with a |Ratio Z| > 3 (Primary criterion). The secondary criterion was |W1 Z|<1 (where the mean and standard deviation were calculated for either each plate or for all the plates run on a given experiment). The "alternative secondary criterion" used the mean and standard deviation for all plates in a given experiment. Compounds with very strong inhibition in the W1 channel were treated as likely TRF-donor quenchers and de-prioritized. Compounds with very bright W2 signal were similarly treated as non-specifically fluorescent compounds. The residual structures of

prospective hit compounds were exported for review by medicinal chemists and analysis through structure activity landscape index (SALI) plots(8). Following the identification of hits based on these parameters, we then designed a custom set of plates with compounds picked from the in house deck. The confirmatory TR-FRET screens were performed in triplicate with further analysis as described in the results section.

Counter-Screen and Cell-based Assays.

A custom set of plates was constructed from the hits that were identified from the initial TR-FRET based assays. Wild type and IGF2BP3-deleted SEM cell lines (6) were treated with compound, grown for 4 days under normal growth conditions, and assayed for cell growth in 384-well plates with CellTiter-Glo, a luminescence-based reagent described previously (1, 6, 9). Fold change from control (i.e., no compound treated wells) was plotted for SEM-WT versus SEM-I3KO. We utilized the cutoffs described in the results section to enable downstream analysis of potential lead compounds.

Synthesis of I3IN-002

Commercially available reagents were used as received. Methanol (MeOH) was purchased from Fischer Scientific. Deionized water was used. Dimethyl sulfoxide (DMSO) was purchased from Sigma-Aldrich. K_2CO_3 was purchased from Oakwood Chemical. 5-Methyl isatin **4** and α-chloro amide **7** were purchased from Combi-Blocks. Thiosemicarbazide (**5**) was purchased from AK Scientific. Reaction temperatures above 23 °C were controlled using an IKAmag temperature modulator, and unless stated otherwise, performed at room temperature (approximately 23 °C). ^{1}H-NMR spectra were recorded on Bruker spectrometers (at 500 MHz) and are reported relative to the residual solvent signal. Data for ^{1}H-NMR spectra are reported as follows: chemical shift (d ppm), multiplicity, coupling constant (Hz), and integration. ^{13}C-NMR spectra were recorded on Bruker spectrometers (at 125 MHz) and are reported relative to the residual solvent signal. Data

for ^{13}C-NMR spectra are reported as follows: chemical shift (d ppm) and, when necessary, multiplicity and coupling constant (Hz). ^{19}F-NMR spectra were recorded on Bruker spectrometers (at 564 MHz) and are reported relative to the residual solvent signal. Data for ^{19}F-NMR spectra are reported as follows: chemical shift (d ppm) multiplicity and integration. IR spectra were recorded on a Perkin-Elmer UATR Two FT-IR spectrometer and are reported in terms of frequency absorption (cm^{-1}). DART-MS spectra were collected on a Thermo Exactive Plus MSD (Thermo Scientific) equipped with an ID-CUBE ion source and a Vapur Interface (IonSense Inc.). Both the source and MSD were controlled by Excalibur software version 3.0. The analyte was spotted onto OpenSpot sampling cards (IonSense Inc.) using CH_2Cl_2 as the solvent. Ionization was accomplished using UHP He plasma with no additional ionization agents. The mass calibration was carried out using Pierce LTQ Velos ESI (+) and (–) Ion calibration solutions (Thermo Fisher Scientific). Retention times for liquid chromatography were recorded with a Shimadzu Nexera XR equipped with a PDA detector. Chromatography was conducted using a 0.5 mL/min flow rate at 40 °C and Shimadzu Nexcol C18 (1.8 x 50 mm, 2.1 µm) column. Two mobile phase solutions were used: solution A 0.1% formic acid in water and solution B was 0.1% formic acid in acetonitrile. The elution program consisted of a linear gradient starting at 95% A 0.5 min following injection to 5% A over 4 min. All the final compounds presented a purity of at least 95%, determined by HPLC and ^{1}H NMR. Uncorrected melting points were measured using a Digimelt MPA160 melting point apparatus.

A round-bottom flask containing a magnetic stir bar was charged with K_2CO_3 (1.52 g, 11.0 mmol, 1.1 equiv), isatin **4** (1.75 g, 10.0 mmol, 1.0 equiv), thiosemicarbazide **5** (911 mg, 10.0 mmol, 1.0 equiv,) and MeOH (17 mL, 0.60 M). The reaction mixture was allowed to stir at 23 °C for 18 h. At this point, the reaction mixture was acidified by dropwise addition of acetic acid over roughly 5 min (5 mL). The resulting mixture was stirred for 1 hour. After 1 h, the mixture was vacuum filtered over a fritted funnel, and the filter cake containing the product was washed with H_2O (100 mL), followed by Et_2O (50 mL) to afford (E)-2-(5-ethyl-2-oxoindolin-3-ylidene) hydrazine-1-

carbothioamide (2.10 g, crude mass) as a yellow-orange solid. This was used directly in the subsequent reaction without further purification.

To a round-bottom flask containing a magnetic stir bar, (E)-2-(5-ethyl-2-oxoindolin-3-ylidene) hydrazine-1-carbothioamide (2.10 g, 8.46 mmol, 1.0 equiv.) and K_2CO_3 (1.17 g, 8.46 mmol, 1.0 equiv) were added, and dissolved in H_2O (100 mL, 0.08 M). The reaction vessel was fitted with a reflux condenser and the reaction mixture was stirred at 100 °C for 16 h. At this point, the crude mixture was allowed to cool to 23 °C. It was acidified by the dropwise addition of acetic acid over roughly 5 min (10 mL) and then stirred for an additional hour. The mixture was vacuum filtered over a fritted funnel, and the filter cake containing the product was washed with H_2O (100 mL), followed by Et_2O (50 mL) to afford triazinoindolothione **6** (1.47 g, 65% yield over two steps, >95% purity) as a yellow-orange solid.

To a 1-dram vial charged with a magnetic stir bar was added triazinoindolothione **6** (50 mg, 0.22 mmol, 1.0 equiv), α-chloroacetamide **7**(52 mg, 0.22 mmol, 1.0 equiv), K_2CO_3 (60 mg, 0.43 mmol, 2.0 equiv), and DMSO (1.1 mL, 0.20 molar). The reaction mixture was allowed to stir at 23 °C for 16 h. The reaction mixture was transferred to a vial containing H_2O (5 mL), which led to the formation of a precipitate. The mixture was sonicated for 5 minutes to afford the crude product as a suspension in water. This mixture was then heated to reflux for ~ 5 seconds to effect partial dissolution, and was then allowed to cool to 23 °C under ambient conditions. The product precipitated and was collected by vacuum filtration over a paper filter. The filter cake was successively washed with H_2O (5 x 1 mL), MeOH (1 x 0.5 mL), and Et_2O (2 x 1 mL) to give **I3IN-002** (42 mg, 45% yield, >95% purity) as a tan solid. **I3IN-002**: Mp: 253 °C; ^{1}H NMR (500 MHz, $(CD_3)_2SO$): δ 12.54 (s, 1H), 9.90 (s, 1H), 8.14 (s, 1H), 7.72 (d, *J* = 7.8 Hz, 1H), 7.68 (t, *J* = 7.8 Hz, 1H), 7.60 (d, *J* = 8.0 Hz, 1H), 7.56 (dd, *J* = 8.3, 1.4 Hz, 1H), 7.51 (d, *J* = 8.3 Hz, 1H), 7.44 (t, *J* = 7.6 Hz, 1H), 4.27 (s, 2H), 2.80 (q, *J* = 7.5 Hz, 2H), 1.27 (t, *J* = 7.6 Hz, 3H); ^{13}C NMR (125 MHz, $(CD_3)_2SO$): δ 167.3, 165.9, 146.6, 141.3, 138.7, 138.4, 135.2, 133.1, 131.2, 129.3, 126.6, 126.3

(q, *J* = 5.0 Hz), 124.0 (q, *J* = 29.6 Hz), 123.5 (q, *J* = 273.4 Hz), 120.1, 117.6, 112.6, 34.5, 28.0, 16.2; ^{19}F NMR (564 MHz, $(CD_3)_2SO$): δ –59.4 (s, 3H); IR (Film): 3263, 2961, 1662, 1536, 1095 cm^{-1}; HRMS-APCI (*m/z)* $[M + H]^+$ calcd for $C_{20}H_{17}F_3N_5OS^+$, 432.11004; found 432.11002; HPLC purity 97 %; R_t = 4.20 min.

In vitro assays for cell viability, cell cycle apoptosis, and proliferation, with small molecule treatment

Cell viability assays were performed using a luminescent assay based on ATP quantitation (CellTiterGlo, Promega, catalog G7571), per manufacturer's protocol. 1500 cells/well (for 384 well format) and 5000 cells/well (for 96 well format) were plated and incubated with different concentrations of small molecule for four days at 37°C in a 5% CO_2 incubator, followed by endpoint assay. For IC_{50} determinations, small molecule was added at concentrations from 50 μM-0.0004 μM, with 2-fold dilutions. For cell cycle analysis, SEM and RS4;11 cells were treated with 5 μM concentration of I3IN-002 and DMSO for 48 hrs. After 48 hrs. cells were harvested, washed with PBS, and fixed in pre-chilled 70% ethanol overnight. Fixed cells were washed with PBS and 350 μL Propidium Iodide staining solution (20 μg/mL of propidium Iodide and 200 μg/mL of DNase free RNase) was added to the cells and incubated for 1 hr. at RT. Stained cells were run on the flow cytometer and analyzed using FlowJo software V10.

Apoptosis

Apoptosis assays were performed using luminescence-based Caspase Glo assay (Promega). Briefly, SEM and RS4;11 cells were treated with 5 μM concentration of I3IN-002 and DMSO for 48 hrs. Post treatment, 100 μL of Caspase Glo reagent was added to each well (1:1) and incubated for 1 hr. at 37 degree Celsius. Plate was read on Varioscan lux microplate reader from Thermo Scientific. The increase in luminescence in I3IN-002 treated cells compared to DMSO

corresponds to an increase in Caspase 3/7 activity. An alternate measurement of apoptosis was performed on the compound treated cells using Annexin V and propidium iodide staining as described previously(1).

Colony formation assay

Colony formation assay with serial replating was performed using murine Lin-MLL-Af4 cells(6). Briefly, 6000 cells were resuspended in 4 mL of Methocult media (M3434, Stem Cell Technologies) with DMSO/I3IN-002. Then, 1.1 mL of the cell suspension was plated in each 35 mm petri dish and incubated for 8 days. After colony counting, colonies were pooled by adding PBS at room temperature, creating a single-cell suspension by gently mixing with a micropipette, and centrifuging at 1200 rpm for 5 minutes. The pellet was resuspended in PBS, and viable cells were counted using Trypan blue. For serial replating, 1600 cells were seeded again following the previously mentioned steps with DMSO and I3IN-002 (10).

Animal Experiments

For in vivo studies, C57BL/6J, B6.SJL-*Ptprc*^{a} *Pepc*^{b}/BoyJ (B6 CD45.1), and B6J.129(Cg)-Gt(ROSA)26Sor$^{tm1.1(CAG-cas9*,-EGFP)Fezh/J}$ (Cas9-GFP, BL/6J) were procured from The Jackson Laboratory. Primary murine leukemia cells (WT and Igf2bp3 KO) as previously described (6) were transplanted into busulfan-conditioned recipients. One week following transplantation, mice were injected with vehicle or I3IN-002, three times a week intraperitoneally, at a dose of 25 mg/kg, for three weeks, with an endpoint at four weeks post-transplantation. The peripheral blood engraftment of the leukemic cells was checked by FACS at week 2 and week 4. Once the peripheral blood engraftment reached >20% at 4 weeks, the experiment was terminated and tissues were harvested to be analyzed by FACS, histology and RT-qPCR. All of the animal experiments received Institutional Animal Research Committee approval at UCLA.

Cellular thermal shift assay (CETSA)

A cellular thermal shift assay was performed on SEM cells treated with the test compound, based on published protocols(11). Briefly, 20 $x10^6$ cells were treated with 25 µM concentration of test compound in 40 mL of complete growth media and incubated for 24 hour. at 37 ˚C in CO_2 incubator, DMSO was used as vehicle control. After incubation, cells were spun down and washed with PBS. Cells were further re-suspended in 1 mL of PBS with 1x protease inhibitor cocktail and 100 uL of cell suspension was distributed in individual PCR tubes. Cells were subjected to thermal denaturation at different temperature ranging from 38 ˚C – 52 ˚C on a thermal cycler for 3 minutes. Thermal treated cells were lysed by flash freeze and thaw cycle in liquid Nitrogen and cleared by centrifugation at 20,000xg for 20 minutes at 4 °C. Lysates were boiled in sample buffer and subjected to western blotting.

Drug Affinity responsive target stability (DARTS) assay

DARTS assay (12) was performed to study direct binding of I3IN-002 with IGF2BP3 protein. Briefly, $5x10^7$ SEM cells were lysed in 1 mL of m-PER buffer (Thermo scientific) and incubated on ice for 10 minutes. After incubation, lysate was centrifuged at 17,000xg for 10 min at 4^0C. The supernatant was transferred to a fresh tube and mixed with one-tenth of the 10x TNC buffer (500 mM Tris-HCl, pH 8.0, 500 mM NaCl and 100 mM $CaCl_2$), followed by protein estimation using the BCA assay. Approximately 50 µg of lysate was incubated with different concentrations of I3IN-002 (DMSO, 25, 50,100, 250 and 500 µM) for 1 hour, followed by pronase (Roche, 10,165,921,001) treatment (1:500) for 30 minutes at room temperature. The pronase activity was quenched by adding a protease inhibitor cocktail. The lysate was then boiled in 2x Laemmli buffer for 10 min at 90^0C and run on SDS PAGE. The membrane was the probed for IGF2BP3 and Actin beta for loading control.

Thermal Shift Assay (TSA)

Thermal shift assay (13) was performed using both full-length IGF2BP3 and RRM1-2 domain of IGF2BP3 purified protein. Briefly, 10 μM of purified protein was incubated with 100 μM of I3IN-002 for 30 minutes at room temperature. SYPRO dye (5000x) diluted in Bis-Tris buffer, pH 6.5 was added to the reaction mix. The reaction was run on a quantitative PCR machine (QuantStudio 3) using melt curve protocol.

Dual Luciferase Assay

Luciferase assay was performed using the Promega Dual-Luciferase Assay system on IGF2BP3 targets: CDK6, BCL2, HOXA9 and BNIP3L. The CDK6 3' UTR cloning was discussed previously (4). For BNIP3L, 486 bp of the BNIP3L 3'UTR beginning at chromosomal position chr8: 26,411,300; for the BCL2 3' UTR, approximately 591 bp beginning at chromosomal position chr18:63,128,033 were cloned into the pmirGlo vector. Next, 293T cells were co-transfected with the pmirGlo reporter construct and IGF2BP3 overexpression vector, with the reporter vector: overexpression vector ratio of 1:10 (50 ng:500 ng). Co-transfections were performed with BioT (Bioland) as per the manufacturer's instructions. Cells were lysed after 48 hours, Firefly and Renilla Luciferase substrate was added, and luminescence was measured on a Varioscan Lux (Thermo Scientific). The ratio of Firefly to Renilla luciferase activity was calculated for all samples and expressed as the Fold change from DMSO treatment for that particular reporter vector.

RNA isolation and qPCR

Previous protocols were adapted for RT-qPCR as standard procedures (7). A full list of RT-qPCR primers are presented in **Supp. Table 4**. For normalization to housekeeping genes, we used RT-qPCR primers for human 18S (or actin) and mouse L32.

RNA Sequencing.

Total RNA was extracted from cell pellets using Qiazol (Qiagen) per manufacturer's protocol with the following modification to include an additional RNA ethanol wash step: after the total RNA was solubilized in ddH_2O, one overnight ethanol precipitation step was included for further purification. Libraries for RNA-Seq were prepared with KAPA mRNA-Seq Hyper Prep Kit. The workflow consisted of mRNA enrichment and fragmentation, first strand cDNA synthesis using random priming followed by second strand synthesis converting cDNA:RNA hybrid to double-stranded cDNA (dscDNA), and incorporating dUTP into the second cDNA strand. cDNA generation was followed by end repair to generate blunt ends, A-tailing, adaptor ligation and PCR amplification. Different adaptors were used for multiplexing samples in one lane. Sequencing was performed on Illumina HiSeq3000 for a SE 1x50 run. Data quality check was done on Illumina SAV. Sample preparation and sequencing were completed by the UCLA Technology Center for Genomics & Bioinformatics (TCGB).

Bioinformatics Methods & Data Analysis

Following completion of sequencing and data quality check, demultiplexing was performed with Illumina Bcl2fastq v2.19.1.403 software. The reads were mapped by STAR 2.7.9a(14) and read counts per gene were quantified using the human genome GRCh38. In Partek Flow, read counts were normalized by CPM +1.0E-4. All results of differential gene expression analysis utilized the statistical analysis tool, DESeq2(15). P-value ($p<0.05$), FDR (<0.05), and fold change (FC>2-fold) filters were applied for differentially expressed gene lists prior to downstream analysis. Multiple testing correction was performed using the Benjamini–Hochberg method. Significant differentially expressed genes have adjusted *P* value =< 0.05 and absolute log2FC >= 1. Enrichment analyses were completed with Metascape (16).

RNA immunoprecipitation

RNA immunoprecipitation assay was performed on SEM cells treated with 5 μM concentration of I3IN-002 and DMSO for 48 hours. After incubation, cells were lysed in a non-denaturing lysis buffer supplemented with protease inhibitor and RNase inhibitor. Lysate was cleared at 12000 rpm for 15 minutes and RIP was performed on the cleared lysate by adding 5 μg of IGF2BP3 antibody/ IgG and 50 μL of Protein G agarose beads and incubated overnight at 4 degree Celsius.

Immunoprecipitation was confirmed by Western Blotting for IGF2BP3. RNA samples were isolated and subjected to either high throughput RNA-seq, or to directed RT-qPCR for known targets of IGF2BP3.

RIP-seq data analysis.

For RIP-seq, paired input and RIP samples were provided to the UCLA TCGB. Libraries for RNA-Seq were prepared with the ABclonal FAST mRNA Library Prep Kit. Following the same initial pipeline as for RNA-seq (see above), read counts were obtained as above. Next, DE-seq2 was used to compare RIP samples against input, for each of the two conditions, control (DMSO) versus I3IN-002 treatment, yielding high-probability enrichments (padj<0.01) and enrichment ratios (fold-changes). These enrichment ratios were compared between conditions to prepare scatter plots as shown. The ratio difference was calculated as enrichment ratio (I3IN-002)-enrichment ratio (DMSO). Genes that were enriched in DMSO-treated samples were compared against genes previously identified as targets of IGF2BP3 by eCLIP-seq analysis of SEM cells(17).

Statistical analysis

Data shown represents mean ± SD for continuous numerical data, unless otherwise indicated. Two-tailed student's *t* tests or one-way ANOVA followed by Bonferroni's multiple comparisons test were performed using GraphPad Prism software and conducted as described in the figure

legends. Survival analyses were performed using Kaplan-Meier method with comparisons made using log-rank tests, followed by Bonferroni's correction for multiple comparisons. A *P* value less than 0.05 was considered significant.

Additional reagents. Additional reagents and kits are listed in **Supp. Table 5**.

References:

1. Jaiswal AK, Truong H, Tran TM, Lin TL, Casero D, Alberti MO, et al. Focused CRISPR-Cas9 genetic screening reveals USO1 as a vulnerability in B-cell acute lymphoblastic leukemia. *Scientific Reports.* 2021;11(1):13158.
2. Sharma G, Tran TM, Bansal I, Beg MS, Bhardwaj R, Bassi J, et al. RNA binding protein IGF2BP1 synergizes with ETV6-RUNX1 to drive oncogenic signaling in B-cell Acute Lymphoblastic Leukemia. *J Exp Clin Cancer Res.* 2023;42(1):231.
3. Cheung LC, de Kraa R, Oommen J, Chua GA, Singh S, Hughes AM, et al. Preclinical Evaluation of Carfilzomib for Infant KMT2A-Rearranged Acute Lymphoblastic Leukemia. *Front Oncol.* 2021;11:631594.
4. Kasai F, Asou H, Ozawa M, Kobayashi K, Kuramitsu H, Satoh M, et al. Kasumi leukemia cell lines: characterization of tumor genomes with ethnic origin and scales of genomic alterations. *Hum Cell.* 2020;33(3):868-76.
5. Lechman ER, Gentner B, Ng SWK, Schoof EM, van Galen P, Kennedy JA, et al. miR-126 Regulates Distinct Self-Renewal Outcomes in Normal and Malignant Hematopoietic Stem Cells. *Cancer Cell.* 2016;29(4):602-6.
6. Lin TL, Jaiswal AK, Ritter AJ, Reppas J, Tran TM, Neeb ZT, et al. Targeting IGF2BP3 enhances antileukemic effects of menin-MLL inhibition in MLL-AF4 leukemia. *Blood Adv.* 2024;8(2):261-75.
7. Palanichamy JK, Tran TM, Howard JM, Contreras JR, Fernando TR, Sterne-Weiler T, et al. RNA-binding protein IGF2BP3 targeting of oncogenic transcripts promotes hematopoietic progenitor proliferation. *J Clin Invest.* 2016;126(4):1495-511.
8. Guha R. Exploring Structure-Activity Data Using the Landscape Paradigm. *Wiley Interdiscip Rev Comput Mol Sci.* 2012;2(6).
9. Tran TM, Philipp J, Bassi JS, Nibber N, Draper JM, Lin TL, et al. The RNA-binding protein IGF2BP3 is critical for MLL-AF4-mediated leukemogenesis. *Leukemia.* 2022;36(1):68-79.
10. Christen F, Hablesreiter R, Hoyer K, Hennch C, Maluck-Bottcher A, Segler A, et al. Modeling clonal hematopoiesis in umbilical cord blood cells by CRISPR/Cas9. *Leukemia.* 2022;36(4):1102-10.
11. Jafari R, Almqvist H, Axelsson H, Ignatushchenko M, Lundbäck T, Nordlund P, et al. The cellular thermal shift assay for evaluating drug target interactions in cells. *Nature Protocols.* 2014;9(9):2100-22.
12. Pai MY, Lomenick B, Hwang H, Schiestl R, McBride W, Loo JA, et al. Drug affinity responsive target stability (DARTS) for small-molecule target identification. *Methods Mol Biol.* 2015;1263:287-98.
13. Wu T, Hornsby M, Zhu L, Yu JC, Shokat KM, and Gestwicki JE. Protocol for performing and optimizing differential scanning fluorimetry experiments. *STAR Protoc.* 2023;4(4):102688.
14. Dobin A, Davis CA, Schlesinger F, Drenkow J, Zaleski C, Jha S, et al. STAR: ultrafast universal RNA-seq aligner. *Bioinformatics.* 2013;29(1):15-21.
15. Love MI, Huber W, and Anders S. Moderated estimation of fold change and dispersion for RNA-seq data with DESeq2. *Genome Biol.* 2014;15(12):550.

16. Zhou Y, Zhou B, Pache L, Chang M, Khodabakhshi AH, Tanaseichuk O, et al. Metascape provides a biologist-oriented resource for the analysis of systems-level datasets. *Nat Commun.* 2019;10(1):1523.
17. Sharma G, Gutierrez M, Jones AE, Kapoor S, Jaiswal AK, Neeb ZT, et al. IGF2BP3 redirects glycolytic flux to promote one-carbon metabolism and RNA methylation. *Cell Rep.* 2025:116330.

Supplemental Table 1. Reagents used in cell culture experiments.

Cell lines		
RS4;11	ATCC	CRL-1873
NALM6	ATCC	CRL-3273
SEM	DSMZ	ACC 546
REH	ATCC	CRL-8286
PER 785	Kids Cancer Centre, UWA, Perth Australia	
KASUMI-2	DSMZ	ACC 526
OCI-AML8227	Princess Margaret Cancer Centre, Toronto, Canada: Kind gift from Dr. John Dick.	
Media and supplements		
IMDM	Gibco	12440046
RPMI 1640	Gibco	11875119
FBS	Gibco	26140079
mSCF	Invitrogen	RP87738
IL-6	Gibco	PHC0065
hFLT-3	Gibco	PHC9415
mTPO	Invitrogen	RP87753
AMEM	Wisent	310-010 CL
BITS 9000	Stemcell Technologies	09500
R&D SCF	R&D Systems	11010SC010
R&D TPO	R&D Systems	288TP005
R&D FLT3-L	R&D Systems	308FK025
R&D IL-6	R&D Systems	206IL050
R&D IL-3	R&D Systems	203IL010
R&D G-CSF	R&D Systems	214CS005

Supplemental Table 2. Antibodies used in FACS, western blot and immunoprecipitation assays.

Antibodies		
Biolegend	105826	APC/Cyanine7 anti-mouse CD117 (c-kit)
Biolegend	118103	Biotin anti-mouse TCR γ/δ Antibody
Biolegend	312225	Brilliant Violet 711™ anti-human CD10 Antibody
Biolegend	157211	Pacific Blue™ anti-mouse CD45 Antibody
Biolegend	101318	PE/Cyanine7 anti-mouse CD16/32 Antibody
Biolegend	108124	PerCP/Cyanine5.5 anti-mouse Ly-6A/E (Sca-1)
Biolegend	343513	APC/Cyanine7 anti-human CD34 Antibody
Biolegend	303521	PerCP/Cyanine5.5 anti-human CD38 Antibody,
Biolegend	135120	Brilliant Violet 605™ anti-mouse CD117 (c-kit) Antibody
Biolegend	109815	Alexa Fluor® 488 anti-mouse CD45.2 Antibody
Biolegend	101215	PE/Cyanine7 anti-mouse/human CD11b Antibody
BD Bioscience	563973	Annexin V BV421
BD Bioscience	556463	Propidium Iodide solution
Proteintech	67447-1-Ig	cmyc monoclonal antibody
Fisher	50-173-2168	HOXA9 Rabbit anti-Human
Fisher	PIPA527978	CDK6 Polyclonal Antibody
Santa Cruz Biotech	sc-2357	mouse anti-rabbit IgG-HRP
Proteintech	146421AP150UL	rabbit anti-human igf2bp3
MBL	RN009P	MBL igf2bp3 rabbit anti-human/mouse
Sigma Aldrich	A5441	Actin beta Ab
Sigma Aldrich	F1804	Anti-FLAG Ab
Proteintech	674471IG150UL	Myc anti-human
Invitrogen	PA527978	CDK6 anti-human
Proteintech	185011AP150UL	HOXA9 rabbit anti-human
Invitrogen	PA527094	BCL-2 mouse anti-human
Proteintech	12658-1-AP	P4HA1 rabbit polyclonal anti-human
Proteintech	22339-1-AP	BTG2 rabbit polyclonal anti-human
Proteintech	12835-1-AP	KDM3A rabbit polyclonal anti-human

Supplemental Table 3. RNA Sequences used in IGF2BP3-RNA time resolved Forester resonance energy transfer assay.

RNA Oligo for FRET	Sequence
Unmethylated	5'biotin- CGU CUC GGA CUC GGA CUG CU-3'
Methylated	5'biotin- CGU CUC GG(m^6A) CUC GG(m^6A) CUG CU-3'

Supplemental Table 4. Quantitative PCR primers for genes assayed.

Gene name	Primer Sequence
Human	
TGFBR2-F	AAGATGACCGCTCTGACATCA
TGFBR2-R	CTTATAGACCTCAGCAAAGCGAC
BNIP3L-F	CAGCAATAATGGGAACGGGG
BNIP3L-R	ATCTTGTGGTGTCTGCGAGC
PAICS-F	CAC AGT GGT CTG AGG AAC AGC
PAICS-R	TAC AAT TCT GGG GCA ACC AGG
HMGA1-F	TTT TTC CTC TGT TCA CAA AC
HMGA1-R	AGC AGC AGC AAT GAC GGA TGT C
P4HA1 F	ATGACCCCTCGGAGACAGAA
P4HA1 R	GCCTCAGCCTTGGTTTTGC
MYC F	CCACAGCAAACCTCCTCACAG
MYC R	GCAGGATAGTCCTTCCGAGTG
CDK6 F	GCTGACCAGCAGTACGAATG
CDK6 R	GCACACATCAAACAACCTGACC
HOXA9 F	TGGACAGACTTAAATGCCCGC
HOXA9 R	TGAACCTATGATTGTAAGGAGCTG
BCL2 F	CGG TGG GGT CAT GTG TGT G
BCL2 R	CGG TTC AGG TAC TCA GTC ATC C
KDM3A F	CAGGAGCCACAGTAGGAGAC
KDM3A R	AGTTTGCCATCTCGCCTTGT
BTG2-F	ACCACTGGTTTCCCGAAAAG
BTG2-R	CTGGCTGAGTCCGATCTGG
RPS18 F	GAGGATGAGGTGGAACGTGT
RPS18 R	GGACCTGGCTGTATTTTCCA
Mouse	
Cdk6 F	TCTCACAGAGTAGTGCATCGT
Cdk6 R	CGAGGTAAGGGCCATCTGAAAA
Bcl2 F	GTC GCT ACC GTC GTG ACT TC
Bcl 2 R	CAG ACA TGC ACC TAC CCA GC
Hoxa9 F	AAAACACCAGACGCTGGAAC
Hoxa9 R	TCTTTTGCTCGGTCCTTGTT
Myc F	ATG CCC CTC AAC GTG AAC TTC
Myc R	CGC AAC ATA GGA TGG AGA GCA
Kdm3a F	TCGGAGACTTCTGGGATGGA
Kdm3a R	TTCAGTTTGCCATCTCGCCT
Bnip3l F	AGACCCGAAAACATCCCACC
Bnip3l R	CAGAAGGTGTGCTCAGTCGT
mRPS32-F	AAGCGAAACTGGCGGAAAC
mRPS32-R	TAACCGATGTTGGGCATCAG

Supplemental Table 5. Source of kits and reagents used as described in methods.

Kits and Reagents		
Promega	G8091	Caspase-Glo(R) 3/7 Assay, 10ml
Promega	G7572	CellTiter-Glo(R) Luminescent Cell Viability, 100m
Corning	21030CV	PBS
Thermo Scientific	EN0531	DNase free Rnase A
Invitrogen	NP0007	Invitrogen™ NuPAGE™ LDS Sample Buffer (4X)
Invitrogen	NP0002	Invitrogen™ NuPAGE™ MES SDS Running Buffer (20X)
VWR	101414-278	PerfeCTa® SYBR® Green FastMix®, ROX™
VWR	101414-106	qScript cDNA SuperMix, 5X, 100 rnxs
Thermo Scientific	78438	Protease inhibitor cocktail
Thermo Scientific	EO0381	RNase inhibitor
Sigma Aldrich	A2220	A2220 - ANTI-FLAG ® M2 Affinity Gel
Qiagen	12162	QIAGEN Plasmid Maxi Kit (10)
Qiagen	217004	miRNeasy Mini Kit (50)
Sigma Aldrich	B2635-10G	Busulfan
Sigma Aldrich	PPB019	Bis-Tris-Bicine-EDTA
Sigma Aldrich	11719408001	Protein A Agarose, 2 mL
StemCell Tech	3434	MethoCult
Promega	E2920	Dual-Glo® Luciferase Assay
Thermo Scientific	PV3965	LanthaScreen™ Tb-Streptavidin